Applied Chemical Engineering (2026) Volume 9 Issue 3 ISSN: 2578-2010 (O)
doi: 10.59429/ace.v9i3.6153

RESEARCH ARTICLE

Remediation of real samples and herbal extracts contaminated with heavy metals using the Nano- Amine extract of peace lily (Spathiphyllum) plant in Thi-Qar governorate, Iraq

Manal Ajeel Abd Al-Sadah*, Aliaa Shakir Abd Al-Amee

Department of Chemistry, College of Science, University of Thi-Qar, Thi-Qar,64001, Iraq

***Corresponding author:** Manal Ajeel Abd Al-Sadah, manal.ajeel@utq.edu.iq

ABSTRACT

This study developed a novel, cost-effective, and may offer an environmentally friendly method for removing heavy metals from real samples (water, plants, and soil) and herbal extracts (black tea, fenugreek, and anise). Copper oxide nanoparticles acted as the main adsorbent (CuO NPs) were biosynthesized using Berberis vulgaris (common barberry) fruit extract and modified with amines extracted from Spathiphyllum leaves; these materials served as effective adsorbents for heavy metal remediation. Characterization studies utilizing UV-Vis spectroscopy, infrared spectroscopy (FT-IR), X-ray diffraction (XRD), scanning electron microscopy (SEM), and atomic force microscopy (AFM) enabled the analysis of the nanomaterials' physicochemical properties. Optimal reaction conditions, including pH, contact time, temperature, and adsorbent dosage, were determined; the best results were achieved at pH 9, a contact time of 30 minutes, a temperature of 60°C, and a nanomaterial dosage of 1 g. The results demonstrated high removal rates for nickel ions: 97% in water samples, 94.5% in soil samples, and 96% in plant samples. Similarly, removal rates for cobalt ions were 97.7% in water samples, 94.8% in soil samples, and 96.9% in plant samples. Regarding vanadium ions, the removal rates reached 94.7% in water samples, 90.8% in soil samples, and 94.8% in plant samples. As for herbal extracts, the highest removal rate for nickel ions was achieved using black tea extract (98.6%); similarly, the highest removal rates for cobalt ions (99.4%) and vanadium ions (97.4%) were also obtained with black tea. Experiments were performed in duplicate (n=2 technical replicates), and the method demonstrated high removal efficiency (90–99%) and consistent results, alongside environmental safety, offering a sustainable alternative to conventional chemical treatments.

Keywords: CuO nanoparticles (NPs); peace lily (Spathiphyllum); plant-amine extract; adsorption; heavy metal removal

ARTICLE INFO

Received: 01 September 2026
Accepted: 04 October 2026
Available online: 29 October 2026

COPYRIGHT

Copyright © 2026 by author(s).
Applied Chemical Engineering is published by Arts and Science Press Pte. Ltd. This work is licensed under the Creative Commons Attribution-NonCommercial 4.0 International License (CC BY 4.0).
https://creativecommons.org/licenses/by/4.0/

1. Introduction

Pollution is one of the most significant challenges facing humanity and the natural world, particularly given the technological advancements accompanying modern life. Pollution manifests in various forms including water, air, and soil contamination resulting from the presence of harmful substances (both organic and inorganic) or from deviations in the levels of certain essential environmental elements beyond their natural ranges. These substances can be toxic to humans and the environment at high concentrations; they can enter the food chain and cause serious problems. Consequently, removing or reducing them helps mitigate pollution risks and protect the environment[1]. Water pollution is classified as a critical environmental issue; the World Health Organization (WHO) defined it in 1961 as any alteration to the physical, chemical, or biological properties of water that changes its state—whether directly or indirectly—rendering it unfit for its intended uses, such as drinking,

domestic consumption, or agriculture[2]. Adsorption is one of the methods employed to treat heavy metal pollution and is considered one of the oldest, most common, and most effective physicochemical processes. This process relies on the adhesion of pollutant molecules or ions to the surface of a solid material known as an "adsorbent"[3]. The method is distinguished by its ease of application and its ability to remove pollutants even at extremely low concentrations. Adsorption is classified into two types based on the nature of the bonding forces between the adsorbent surface and the adsorbate: physisorption (physical adsorption), which occurs due to van der Waals forces between molecules and the surface and is a reversible process; and chemisorption (chemical adsorption), which occurs when strong chemical bonds form between the pollutant and the adsorbent surface, a process that is often irreversible. Various models describe the adsorption process such as the Langmuir and Freundlich models, helping researchers understand the adsorption mechanism and evaluate its efficiency[4].In this context, Srinam Padmanabhan conducted a 2024 study titled "Adsorption of Heavy Metals from Aqueous Solutions Using Plant-extract Nanomaterials." This study investigated the potential of plant-extract-derived nanomaterials to remove heavy metals from water; the results showed high efficiency in adsorbing lead, cadmium, and nickel. The study also recommended using these nanomaterials as an eco-friendly alternative for treating water contaminated with heavy metals[5] . Another study conducted by Farid Ahmadu in 2018, titled "Chemical Analysis and Characterization of Trace Elements in Black Tea, Green Tea, and Dried Herbs in Nigeria," analyzed samples of black tea, green tea, and herbs, revealing the presence of nickel, vanadium, lead, and cadmium. The results also indicated that black tea contains relatively lower levels of these elements than green tea and herbal teas; nevertheless, it remains a significant indicator of daily exposure[6]. Furthermore, a study conducted by Ibtihaj (2016) in the Al-Shatra district of Iraq aimed at assessing the concentrations of certain heavy metals in selected soil samples revealed notably high levels of lead, cadmium, and nickel across all surveyed areas, pointing to clear soil contamination resulting from human and industrial activities in the region.

2. Materials and methods

2.1. Materials used

Copper Sulfate Pentahydrate ($CuSO_4.5H_2O$, BDH), Hydrochloric acid (BDH), perchloric acid (Sigma Aldrich), Ethanol (BDE), Chloroform (Sigma Aldrich), Sodium hydroxide (Merck). All chemicals were of analytical grade and were used without further purification.

2.2. Instruments

UV-Vis spectrophotometer (Germany-PG (T60UV)), FT-IR Spectrometer, X-ray (shimadzu, Japan), diffractometer (XRD) (Philips-pw1730), Scanning electron microscope(SEM) (TESCAN Miar3), atomic force microscope (AFM) (Core AFM2023 Nanosurf), centrifuge (Model200EPA, Germany), and ultrasonic bath (Germany).

2.3. Preparation of extract from berberis vulgaris fruit

Fresh Berberis Vulgaris fruits were collected from their natural habitat. The Berberis plant serves as a rich natural source of bioactive compounds such as phenolics, flavonoids, and terpenoids that act as reducing and stabilizing agents; furthermore, the objective is to develop an eco-friendly synthesis method utilizing a plant-based source., washed thoroughly with deionized water to remove dirt and dust. They were left to air-dry for two weeks at room temperature, then thoroughly ground using an electric grinder. An aqueous extract of Berberis Vulgaris was then prepared using 18 g of the plant powder, placed in a 1000 mL conical flask, and 600 mL of deionized water was added. The mixture was heated for 30 minutes at 70°C with continuous stirring. The heater was turned off after 30 minutes, and the mixture was stirred for one hour. The mixture was then given some time to settle. Whatman No.1 filter paper was used to filter the stabilized extract. It was stored in the refrigerator at 4°C. The preparation was then used to synthesize nanoparticles.

2.4. Preparation of copper oxide nanoparticles

The CuO nanoparticles (NPs) were synthesized using Berberis fruit extract as a reducing and capping agent. An aqueous solution of copper (II) sulfate pentahydrate (0.2 M) was prepared by adding 4.98 g of $CuSO_4 \cdot 5H_2O$, then adding 100 mL of deionized water. The mixture was then shaken to obtain a homogeneous solution. Then CuO nanoparticles were prepared by mixing 200 ml of copper (II) sulfate pentahydrate solution at a concentration of 0.2 M with 200 mL of Berberis plant extract with continuous stirring at a temperature of 70 °C for two hours. NaOH was added in droplets to the solution to adjust the acidity function (pH 9). The mixture was then left to settle at room temperature for 24 hours and then centrifuged for 20 minutes at 2000 rpm. After that, the precipitate formed was separated and washed with deionized water and ethanol. The precipitate was then dried in an oven at a temperature of 100 -110 °C and stored in an airtight container.

2.5. Preparation of amines extract from peace lily (Spathiphyllum)

Amines were extracted from Spathiphyllum wallisii leaves following the method of Al-Samarrai (1983), modified from Harborne (1973), was used to prepare the amino extract from the peace lily (Spathiphyllum wallisii). This involved placing 10 g of the plant powder in the extraction thimble of a Soxhlet apparatus, adding 200 mL of 96% ethyl alcohol, and conducting the extraction for 24 hours at 40- 45°C. The filtrate was then concentrated using a rotary evaporator at 40-45°C until it reached a gummy consistency. The sample was then dried in an electric oven at 40-45°C. The dried material was dissolved in 5 mL of ethyl alcohol solution, and 30 mL of 2% sulfuric acid was added to the alcoholic extract. Finally, sufficient quantities of 10% ammonium hydroxide (NH_4OH) were added to this solution to achieve the desired concentration. The (pH =9), the basic solution was placed in the separation funnel and (10 mL) of chloroform was added to it. The mixture was shaken several times and left to separate into two layers. The lower layer (containing the endogenous amines in the chloroform) was taken and the upper layer was discarded. The last step was repeated three times and the lower layer was taken each time so that the volume of the collected solution became (40 mL). Then the sample was dried in the oven at a temperature of (40-45) ℃ and the dry material was stored in a tightly sealed glass container and kept in the refrigerator until use. The extraction process was repeated several times to obtain a sufficient quantity of amines.

2.6. Promoted adsorbent of plant amines with copper oxide nanoparticles

One gram of copper oxide (CuO NPs) was placed in a 100 mL flask, and 10 mL of deionized water was added. The suspension was placed in an ultrasonic device for a sufficient time to ensure homogeneous particle distribution. An amine solution was also prepared by dissolving one gram of amines from a plant source in an appropriate amount of deionized water. The nanosuspension was then mixed with the amine solution at a 1:1 ratio, and the pH was adjusted (pH = 7) using a buffer solution. The amine solution was gradually added to the CuO NPs suspension while stirring with a magnetic stirrer to ensure a good reaction at 40–45 °C for 30 minutes. The precipitate was then filtered and washed twice with deionized water and once with ethanol. Finally, it was dried in an oven at 60 °C. The resulting nano- adsorbent amine was obtained and stored for further use[8].

2.7. Preparation of standard solution of heavy metal (V^{+5}, Ni^{+2}, Co^{+2})

For the purpose of conducting an analytical study, both (V^{+5}), (Ni^{+2}), and (Co^{+2}) were prepared at a concentration of 1000 ppm by dissolving (0.0426 g), (0.049 g), and (0.047 g) of vanadium(V) sulfate trihydrate, nickel (II) nitrate hexahydrate, and Cobalt (II) Sulfate heptahydrate, respectively, using deionized water in a 100 mL volumetric flask. The volume was then topped up to the mark with deionized water. From these concentrations, a series of other dilute solutions of vanadium, nickel, and cobalt were prepared.

2.8. Determining the optimal conditions for heavy metal removal using a nano-adsorbent amine

To determine the optimal conditions, 10 mL of a standard solution containing known concentrations of the heavy metals Ni^{+2}, V^{+5}, and Co^{+2} was taken and placed in a 15 mL centrifuge tube. 0.5 g of plant-extract nano-Adsorbent Amines was added, and the mixture was shaken manually or agitated for two minutes to obtain a homogeneous solution. The pH of the solution was then adjusted to the desired value (pH =9). The tube was then placed in an ultrasonic device for 10 minutes. The ultrasonic vibrations equilibrated the two phases, allowing ion adsorption onto the surface of the nanomaterial. The solid phase was separated from the liquid phase by centrifuging the tube at 4000 rpm for 10 minutes, and the results were then measured using a spectrophotometer[5] .

2.8.1. Effect of pH

In three 15 mL volumetric bottles, each containing 10 mL of vanadium or nickel, Cobalt solution at a concentration of 1 ppm, 0.5 g of nano- Adsorbent amines were added, and the pH was adjusted to different values (pH = 3, 7, 9). The solution was then mixed and diluted to the mark with deionized water. The mixture was then centrifuged at 5000 rpm for 10 minutes, and the result was measured using a spectrophotometer[5] .

2.8.2. Effect of temperature

Three 15 mL volumetric bottles, each containing 10 mL of vanadium or nickel Cobalt solution at a concentration of 1 ppm, were prepared. Then, 0.5 g of nano-Adsorbent amines was added, and the pH was adjusted to optimum values. The bottles were then left at different temperatures (5, 25, and 60 °C), mixed, and diluted to the mark with deionized water. The mixture was then centrifuged at 5000 rpm for 10 minutes, and the resulting mixture was measured using a spectrophotometer[5].

2.8.3. Effect of adsorbent dosage

In three 15 mL volumetric bottles, each containing 10 mL of vanadium or nickel Cobalt solution at a concentration of 1 ppm, different concentrations (1 g, 0.1 g, 0.5 g) of nano-Adsorbent amines were added, maintaining all optimal conditions. The mixture was then centrifuged at 5000 rpm for 10 minutes, and measurements were taken using a spectrophotometer[5] .

2.8.4. Effect of contact time

In three 15 mL volumetric bottles, each containing 10 mL of heavy metal solutions, 0.5 g of nano-Adsorbent amine was added while maintaining optimal conditions of pH, temperature, and substance concentration. Different time intervals (10 min, 30 min, 120 min) were selected to determine the optimal time, and the contents were centrifuged at 5000 rpm for 10 min[5] .

2.9. Preparation of herbal extracts

Commercially available herbal extracts, including fenugreek, anise, and black tea, were used. These extracts were finely ground using an electric grinder to obtain a homogeneous, fine powder. 10 g of each herbal extract was weighed and dissolved in 100 mL of deionized water with continuous stirring to ensure complete dissolution. This solution was divided into two 50 mL portions. The first served as an untreated control sample, while the second was treated by adding 1g of the nano-Adsorbent active ingredients. Both vials were held steady for 30 minutes under optimal conditions. They were then centrifuged for 10 minutes at 5000 rpm, filtered to remove suspended particles, concentrated using a rotary evaporator, dried to obtain a solid precipitate, and then reconstituted with distilled water for measurement[5] .

2.10. The area of the study

The Dhi-Qar Governorate is located in southern Iraq, approximately 360 km southeast of Baghdad, between latitude 31°23′ N and longitude 46°15′ E, and covers an area of about 12,900 km². To ensure the

reduction of several administrative issues such as photography, favors, and reforms, the region is characterized by a hot, dry climate in summer and a mild climate in winter with limited rainfall. The Euphrates River flows through the area, providing water resources for agriculture and domestic use. Due to its industrial and agricultural impact, the region faces challenges in its green spaces, including water and soil enrichment with minerals, making it a suitable model for small plants[9].

2.11. The collection of samples

Samples were collected from different areas in Dhi-Qar Governorate, Iraq (Al-Gharraf, Al-Fadhiliya, and Nasiriyah) during the same growing season in November 2025 to ensure uniformity of environmental conditions. Okra plant samples were collected and placed in clean, tightly sealed bags, each labeled with information regarding the collection site, plant type, and time. Soil samples were also collected from the same site as the plant samples. This selection of the same location aimed to compare heavy metal accumulation. Water samples were also collected from the same site. Water samples used for soil analysis were placed in tightly sealed plastic bottles to prevent external contamination until use.

2.12. Digestion of samples

The digestion method is used to analyze soil and plant samples, using a mixture of nitric acid (HNO_3) and perchloric acid ($HClO_4$). This mixture is effective for breaking down organic and mineral matter. 1g of each sample is placed in a 50 mL crucible. Initial digestion is performed by adding 10 mL of concentrated nitric acid to the sample. The crucible is then placed on a hot plate for 30 minutes to allow initial oxidation. After cooling, 5 mL of perchloric acid (70%) is added to the crucible, and it is reheated until the solution becomes clear and almost dry, indicating complete digestion. The sample is then cooled and filtered using Whatman filter paper (No. 42). The filtered solution is transferred to a 25 mL volumetric flask, and the volume is then filled to the mark with deionized water. Finally, the solution is analyzed using flame atomic absorption spectroscopy[9].

2.13. Reproducibility and control samples

Each measurement was repeated twice (n= 2) using the same prepared sample to verify accuracy and reproducibility (technical replicates). Blank samples (without adsorbent) were used as controls to compare adsorption efficiency.

3. Results and discussion

3.1. Chemical analysis of prepared CuO nanoparticles

3.1.1. FT-IR spectrum of CuO nanoparticles

The FT-IR spectra for the Berberis vulgaris plant extract and the copper oxide nanoparticles are shown in Figures 1and 2. The plant extract exhibited absorption peaks at 3414 cm^{-1} (attributed to O-H stretching vibrations) and 2929 cm^{-1} (attributed to C-H stretching vibrations), as well as peaks at 1737 cm^{-1} (attributed to C=O stretching vibrations); these indicate the presence of hydroxyl, aliphatic, and carbonyl groups that act as reducing and stabilizing agents during nanoparticle formation. Regarding the FT-IR spectrum of the copper oxide nanoparticles, a broad band is observed between 3427 cm^{-1} and 3741 cm^{-1} (attributed to O-H stretching vibrations), and a peak at 2877 cm^{-1} (attributed to C-H stretching vibrations); vibrations at 1616 cm^{-1} (attributed to C=O stretching) indicate the presence of organic groups from the plant extract on the nanoparticle surface. Additionally, characteristic peaks appeared in the 455– 617 cm^{-1} range, attributed to the Cu-O bond, confirming the successful formation of copper oxide nanoparticles[10] , as shown in **Table 1** and **Figures 1 and 2**.

Table 1. Represents the most important bands appearing in the FT-IR of the plant extract and the nanomaterial.

Material	μ(O-H)	μ(C-H)	μ(C=O)	μ(C-O)	μ(C=C)	μ(Cu-O)
Plant Extract	3414	2929	1737	1097	1516	-----
CuO (NPs)	3741-3427	2877	1616	1074	1550	455-617

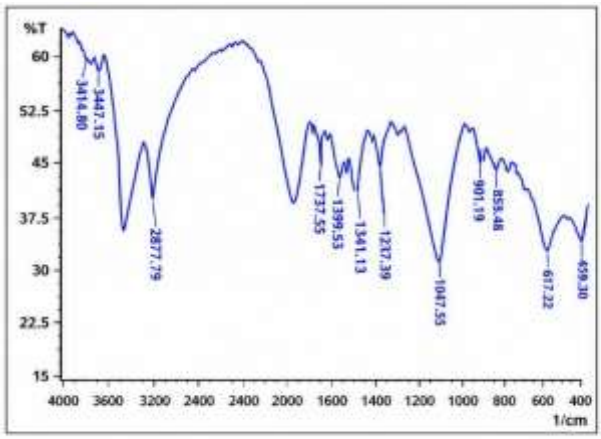


Figure 1. FT-IR of Plant Extract

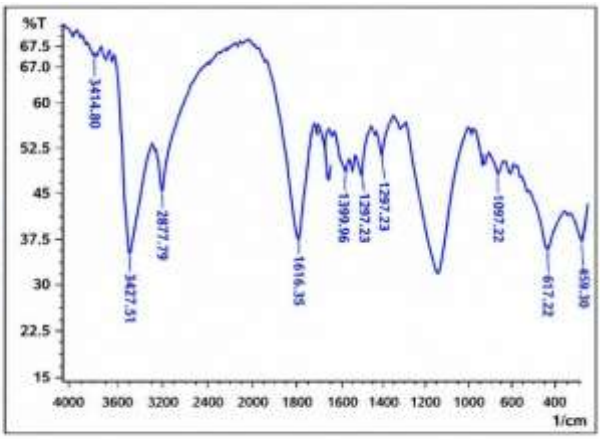


Figure 2. FT-IR of CuO NPs

3.1.2. UV-Vis Spectrum of CuO Nanoparticles

The absorption spectrum of the prepared copper oxide nanoparticles was measured using UV-Vis spectroscopy at different wavelengths within the range of 200–800nm. The UV-Vis spectrum of CuO NPs showed absorption peaks at 270–295nm, representing electron transfer from oxygen (O_2) to copper (II) (Cu^{2+}) within the copper oxide lattice. This absorption indicates the presence of strong Cu–O bonds and is evidence of the formation of a CuO NPs crystalline structure. Two absorption peaks were also observed: a primary peak at 281nm and a smaller peak at 372 nm, indicating the presence of CuO nanoparticles. This is consistent with previous studies[11], as shown in **Figure 3.**

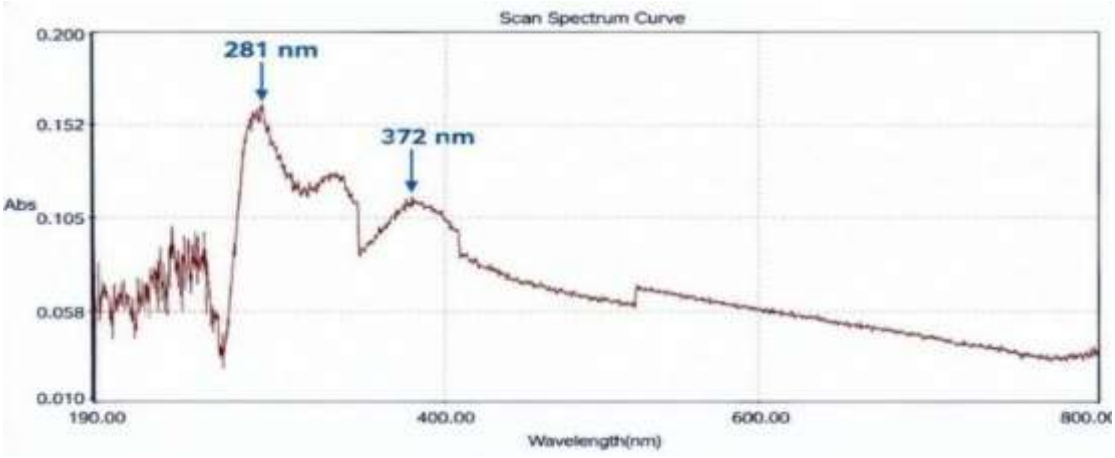


Figure 3. UV-Vis spectrum of CuO NPs.

3.1.3. X-ray diffraction (XRD)

Copper oxide nanoparticles (CuO NPs) were analyzed using X-ray diffraction (XRD) to determine their crystal structure and crystal size. The spectrum showed diffraction peaks at (2θ°) angles of 32.10°, 35.40°, 38.20°, 41.48°, 53.50°, and 61.20°, which correspond to the (110), (002), (111), (131), (123), crystal planes,

respectively[12] . These peaks indicate the formation of a highly crystalline material with a characteristic crystalline quality. The average crystal size was calculated using the Scherrer equation and was found to be equal to 21.4nm, confirming the stable nanoscale nature of the prepared particles[13] , as shown in **Figure 4.**

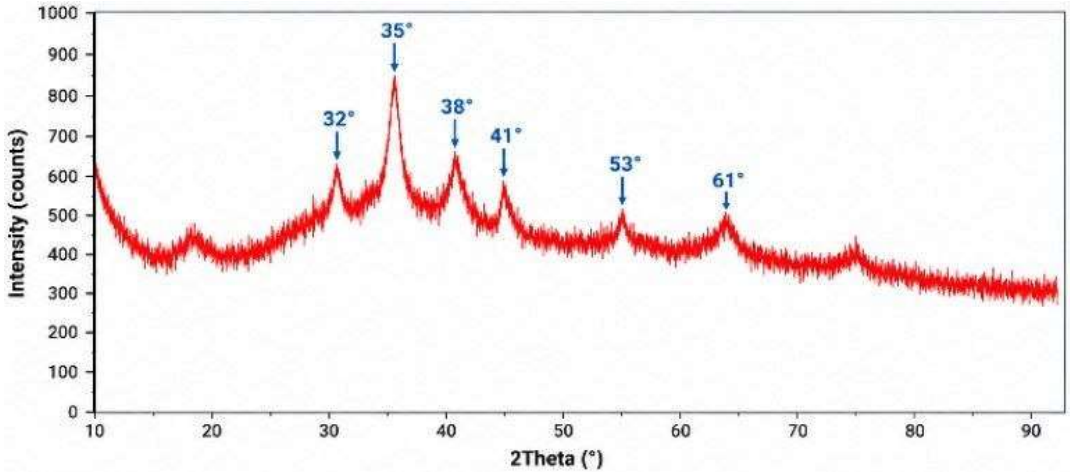


Figure 4. X-ray diffraction of prepared CuO NPs.

3.1.4. FE-scanning electron microscopy (FE-SEM)

Scanning electron microscopy (SEM) is a versatile tool widely used to observe the surface features of materials and provides information about the size and shape of nanoparticles. SEM images of copper oxide nanoparticles in the (36-56) nm range show a rough, heterogeneous surface structure with some aggregates and distinct cracks. These results confirm the nanoscale nature of the material and illustrate the small particle size and large specific surface area, making it useful in applications requiring large surface interactions[14] , as shown in **Figure 5.**

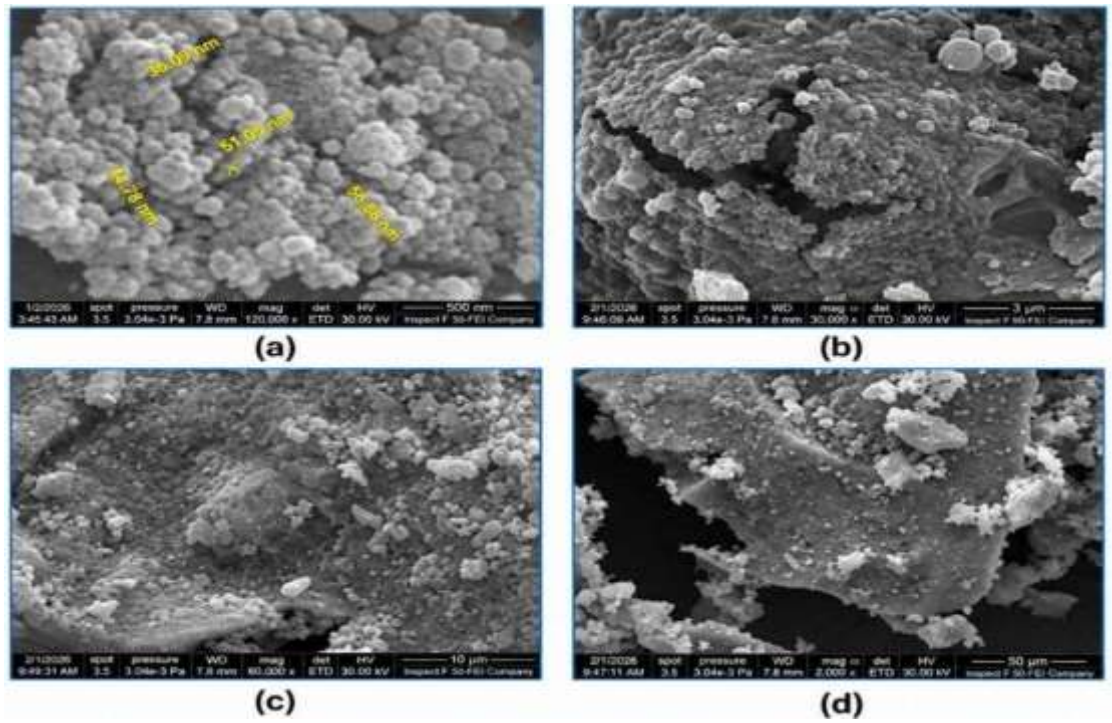


Figure 5. Scanning electron microscopy of prepared CuO NPs.

3.1.5. Atomic force microscopy (AFM)

Copper oxide nanoparticles (CuO NPs) were analyzed using atomic force microscopy (AFM). Threshold detection revealed 668 particles with a surface coverage of 51.15%, an average diameter of 66.49 nm, and a

maximum height of 322.5 nm, indicating a dense and homogeneous distribution and the surface morphology observed by AFM indicates a relatively large surface area. Roughness parameters showed that the average surface height Sa= 16.59 nm and standard deviation Sq= 23.19 nm indicate moderate nano-roughness, with maximum values of Sp = 200.8 nm and Sv = 57.58 nm, and a maximum height range of Sz = 258.3 nm. Positive values for the standard deviation Ssk = 1.895 and the kurrhagia Sku = 11.87 indicate that the surface has more ridges than pits, with sharp peaks, which supports the surface activity of the nanomaterial[15], as shown in **Figure 6**.

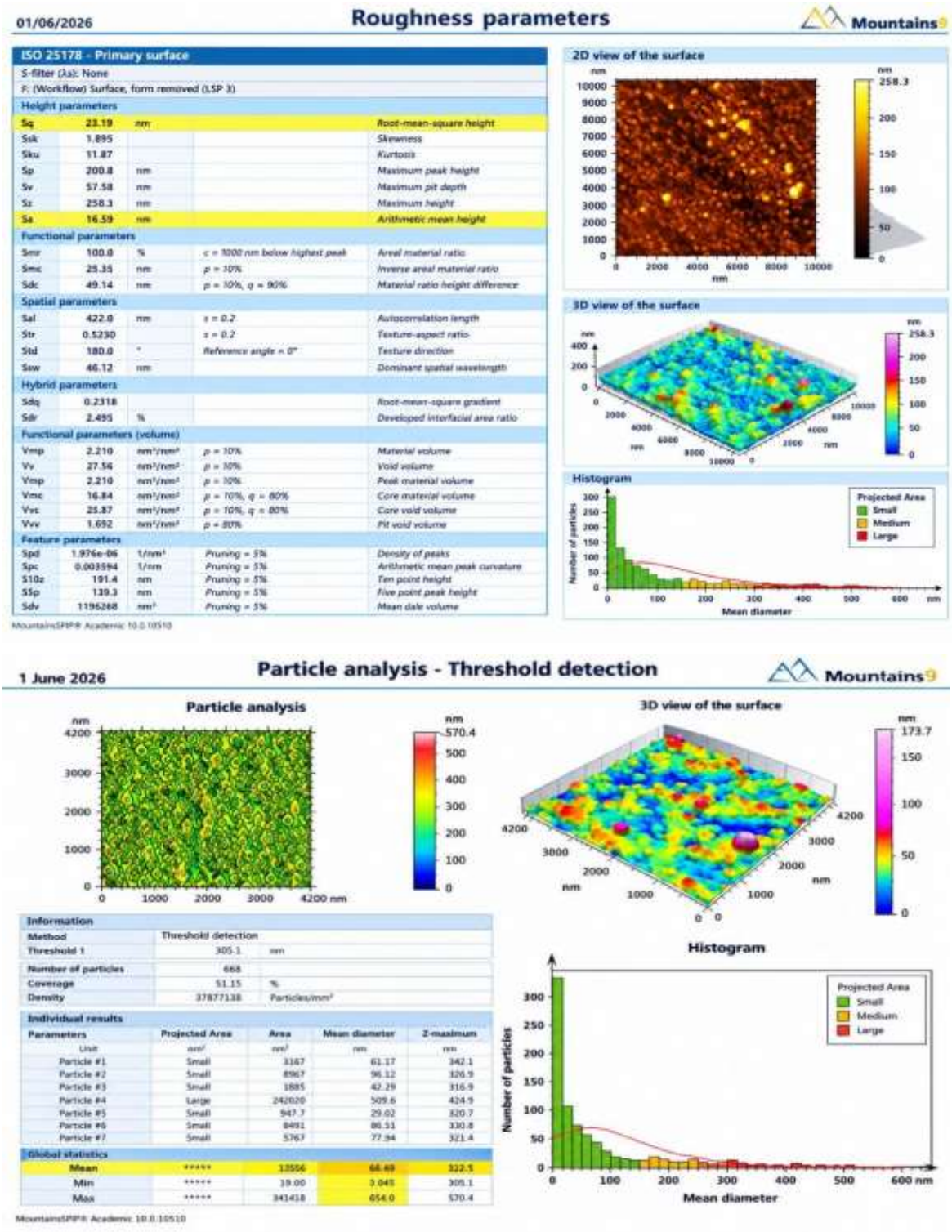


Figure 6. Atomic force microscopy of prepared CuO NPs.

3.2. Chemical analyses of the peace lily extract (Spathiphyllum)

3.2.1. UV-Vis spectrum

The UV-Visible absorption spectrum of the amine extracted from the peace lily plant was recorded within the 200–800 nm range. A single major peak is observed between 240 and 260 nm (at an absorbance of 0.752), associated with the characteristic range for n $\rightarrow \pi *$transitions in N-H and C-N bonds; this indicates the presence of amine compounds in the extract. Furthermore, the broad shape of the peak suggests that the extract contains a mixture of other active compounds, such as phenols and flavonoids[16] , as shown in **Figure 7**.

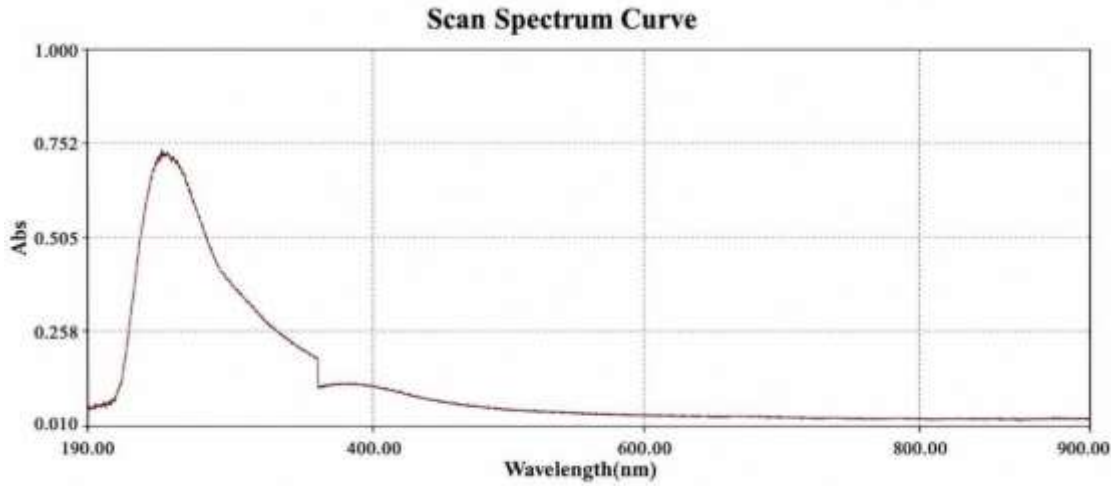


Figure 7. UV-Vis of plant-amine extract of peace lily (Spathiphyllum).

3.2.2. FT-IR Spectrum

FT-IR spectroscopy is a powerful analytical tool for identifying functional groups in organic compounds. In the amine extract of the peace lily plant, a broad absorption band appears in the 3026–3207 cm^{-1} range, attributed to the N–H stretching vibrations of amines; the breadth of this band and the lack of resolved peaks within it result from the overlap of the amine with other compounds present in the plant extract. Additionally, bands appear between 1627 and 1739 cm^{-1}, attributed to C=O or C=N stretching vibrations associated with amines, as well as bands in the 1404–1508 cm^{-1} range corresponding to C=C stretching vibrations in aromatic rings. Bands are also observed at 1111 cm^{-1} (attributed to C–N) and at 833 cm^{-1} attributed to out-of-plane C–H vibrations[17] , as shown in **Figure 8.**

Table 2. Represents the most important bands appearing in the FT-IR of the plant extract.

Material	μ(N-H)	μ(C=O)	μ(C=C)	μ(C-O)	μ(C-H)
Plant Extract	3207-3026	1739-1627	1404-1508	1111	833

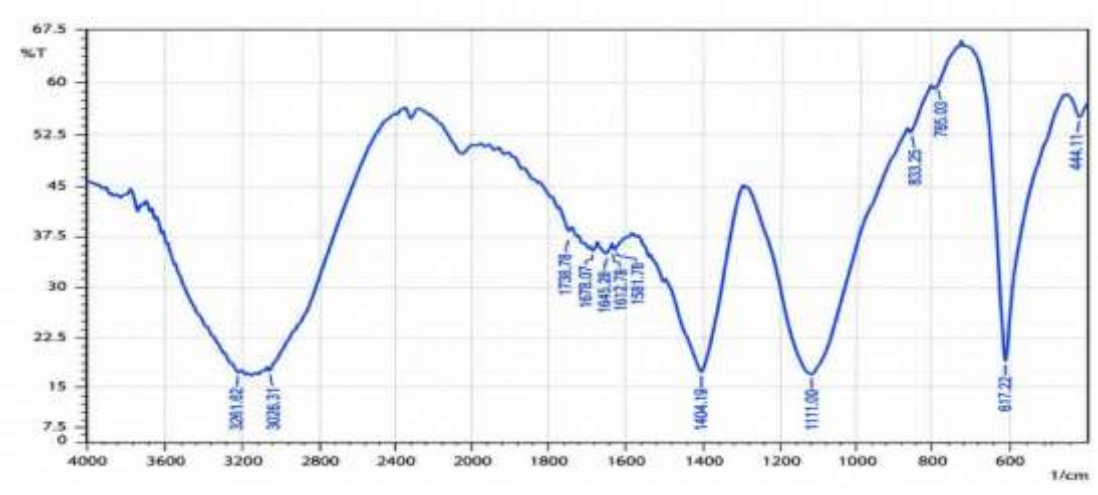


Figure 8. FT-IR of plant-amine extract extracted from peace lily (Spathiphyllum).

3.3. Chemical analysis of the nano-adsorbent plant extract

3.3.1. UV-Vis spectrum

The UV-Visible spectrum of the Nano- Adsorbent Spathiphyllum (Peace Lily) plant extract recorded within the 200–400 nm range reveals distinct changes in peak position, absorption intensity, and band width compared to the spectra of the plant extract or the nanoparticles alone. The spectrum displays a primary absorption peak spanning from 190 nm to 350 nm, with an absorbance value of 0.775; this indicates electronic interactions between the amine groups and the nanoparticles. This shift in absorption confirms the formation of a stable nanocomposite resulting from the reaction between the amine and the CuO nanoparticle surface[18] , as shown in **Figure 9**.

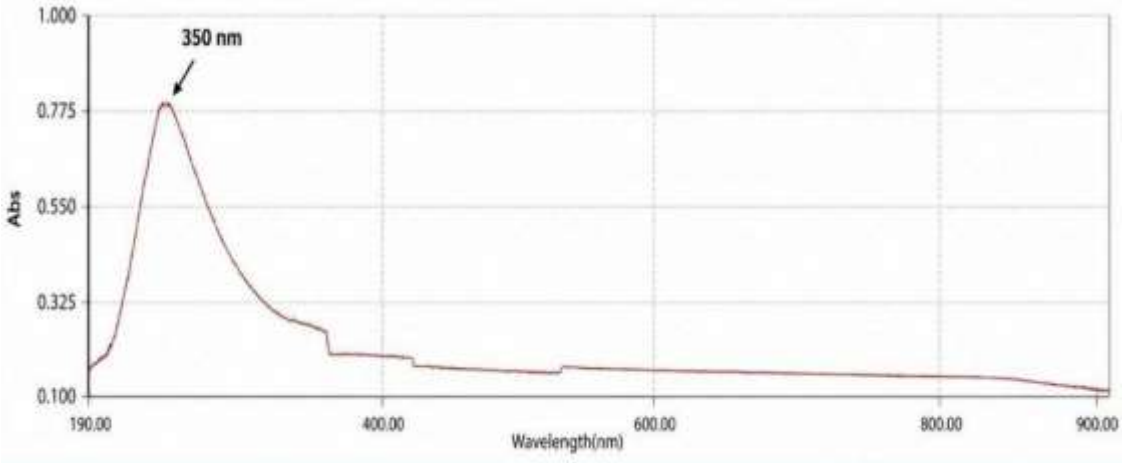


Figure 9. UV-Vis for the nano-adsorbent plant extract.

3.3.2. FT-IR spectrum

The Nano-Adsorbent plant extract was analyzed using infrared (FT-IR) spectroscopy to identify active functional groups. The results revealed characteristic peaks at 3250 cm^{-1}, attributed to N-H vibrations indicating the presence of amines; peaks in the 1689–1791 cm^{-1} range, attributed to C=O vibrations indicating carbonyl groups or coordination bonds with copper; and bands in the 1585–1593 cm^{-1} range, attributed to C=C vibrations in aromatic compounds. Additionally, bands at 1093 cm^{-1} (attributed to C-N vibrations) confirmed the formation of new amine bonds, while low-intensity bands in the 615–815 cm^{-1} range (attributed to Cu-O vibrations) indicated the binding of amines to CuO nanoparticles[19] , as shown in **Figure 10.**

Table 3. Spectral bands of FT-IR Nano - Adsorbent plant extract.

Material	μ(N-H)	μ(C=O)	μ(C=C)	μ(C-O)	μ(Cu-O)
Nano-Adsorbent Plant Extract	3250	1791-1689	1593-1585	1093	815-615

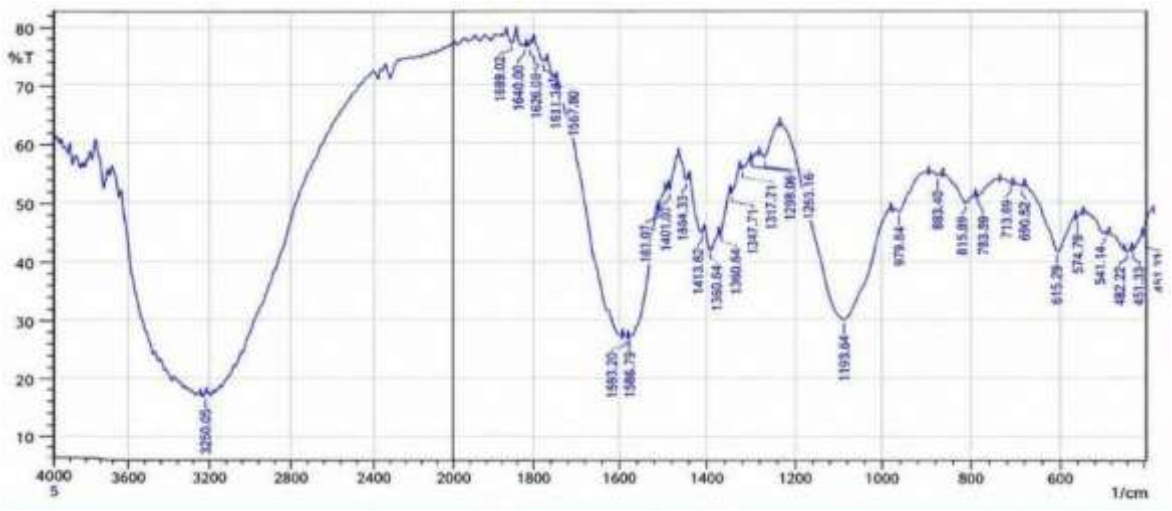


Figure 10. FT-IR of the Nano- Adsorbent plant extract.

3.4. Determination of calibration curve for vanadium, nickel and cobalt ions

To determine the standard calibration curve for vanadium, nickel, and cobalt ions, several solutions were prepared with concentrations ranging from (2-10) μg.mL^{-1} for each ion. Absorption values were recorded at the maximum wavelengths of vanadium 760 nm, cobalt 510 nm, and nickel 398 nm.

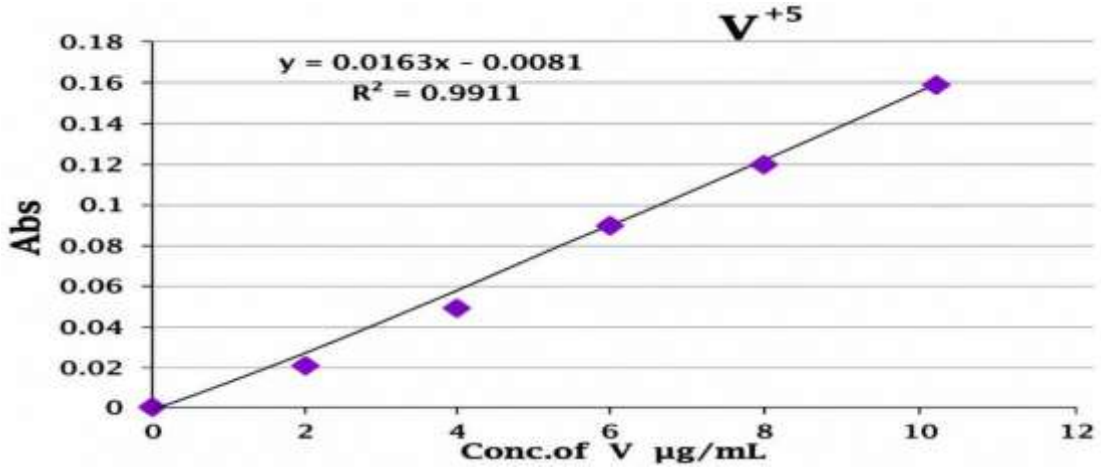


Figure 11. Standard calibration curve for vanadium ion.

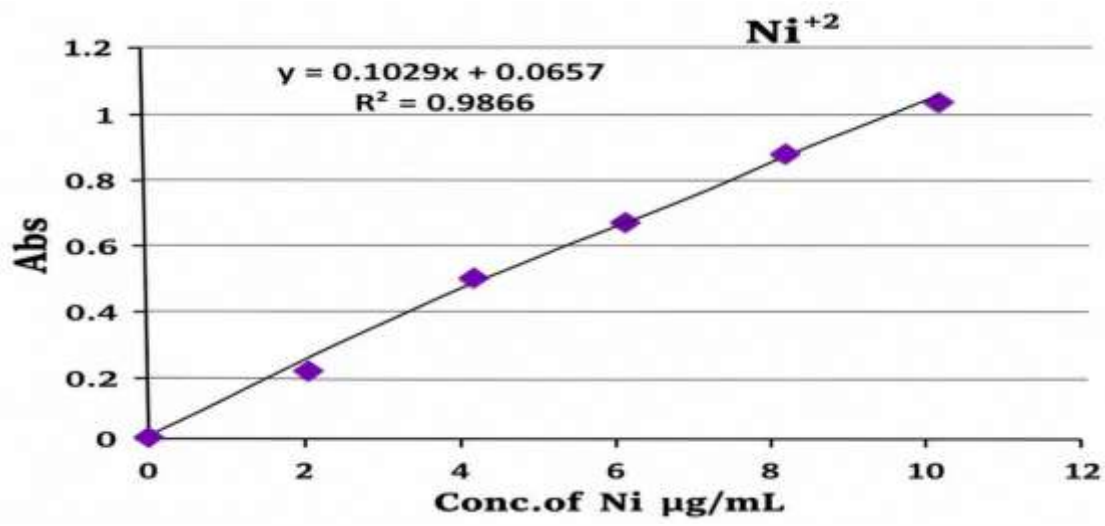


Figure 12. Standard calibration curve for Nickel ion.

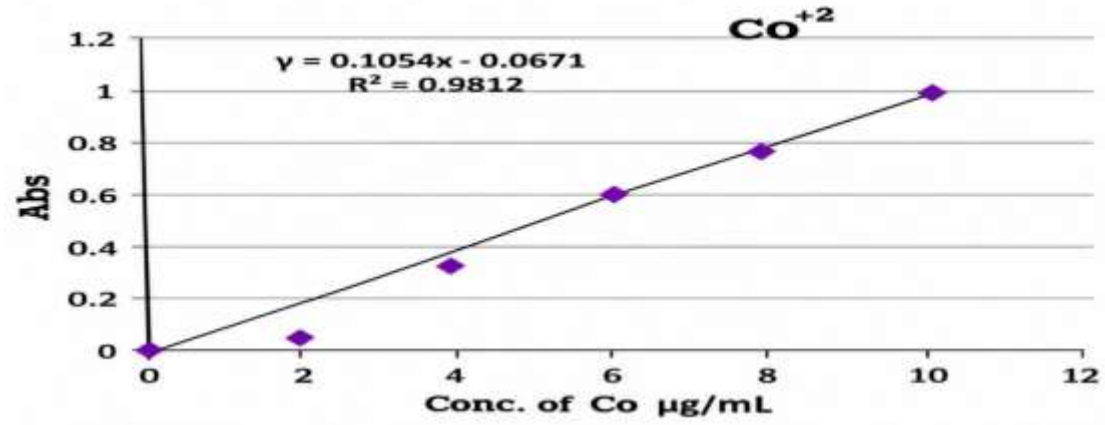


Figure 13. Standard calibration curve for cobalt ion.

Calibration curves were plotted for vanadium (V^{+5}), nickel (Ni^{+2}), and cobalt (Co^{+2}) ions using standard solutions with concentrations ranging from 2 to 10 µg/mL. The resulting equations were:

V^{+5}: $y = 0.0163x - 0.0081$, $R^2 = 0.9911$

Ni^{+2}: $y = 0.1029x + 0.0657$, $R^2 = 0.9866$

Co^{+2}: $y = 0.1054x - 0.0671$, $R^2 = 0.9812$

Measurements were performed in triplicate using the calibration curves, and the standard deviations were less than 0.02 absorbance units, confirming the accuracy of the analytical measurements.

3.5. Determining the optimal condition for heavy metal removal using Nano-Adsorbent amine

3.5.1. Effect of pH

The pH of a sample solution is one of the most important factors affecting the efficiency of heavy metals removal from aqueous solutions of real samples, as it directly affects the ion configuration. The effect of pH on the removal of Ni^{+2}, V^{+5}, and Co^{+2} ions was studied at different values (pH=9, pH=7, and pH=3). This study aimed to determine the optimum pH, which was found to be at its highest value at pH=9, This is because, at pH 9, the surface charges of the particles are negative, which enhances the attraction of positively charged metal ions; experiments have also shown that the highest removal efficiency occurs at pH= 9, due to the balance between solubility and the stability of the prepared particles. Where the ions are in their optimal state[20].

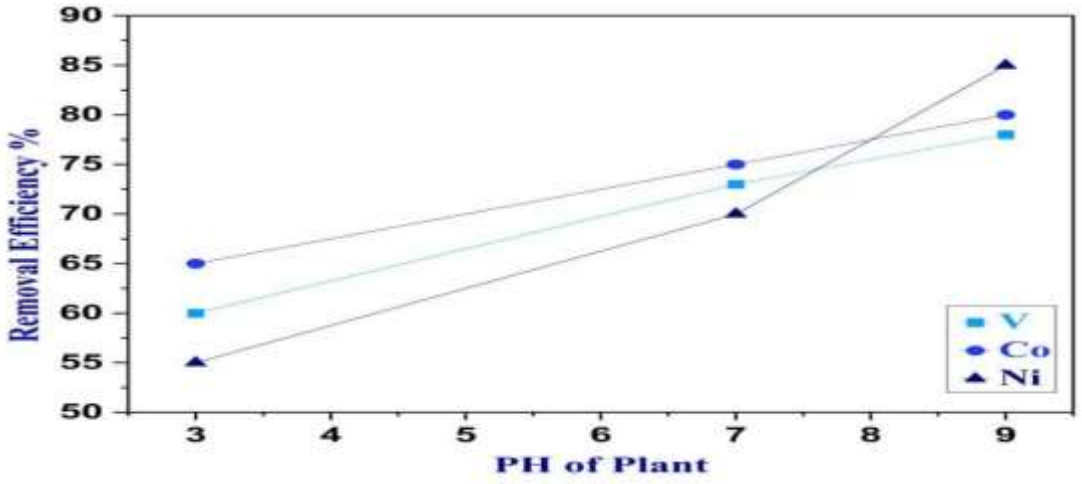


Figure 14. Effect of pH on metals removal efficiency.

3.5.2. Effect of Temperature

The effect of temperature on the removal of heavy metals was studied at three different temperatures (60, 25, 5)℃ , where we note that heating led to an increase in removal efficiency. This is attributed to the fact that increasing the temperature leads to an increase in the kinetic energy of the metal ions in the solution. The optimum value was reached at a temperature of (60℃), Increasing the temperature enhances molecular motion and reduces free energy, thereby increasing the rate of adsorption[21].

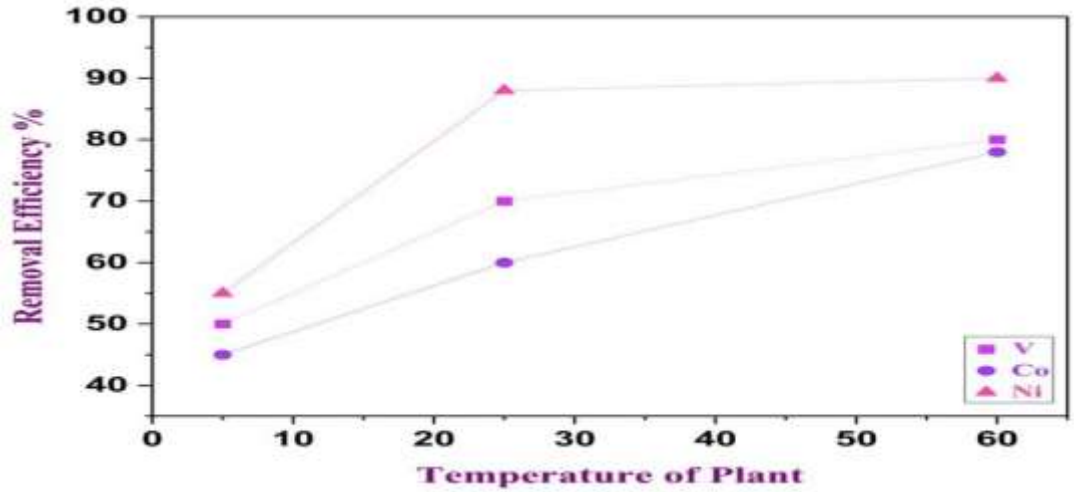


Figure 15. Effect of temperature on metals removal efficiency.

3.5.3. Effect of adsorbent dosage

The concentration of the nanomaterial is a crucial factor affecting the efficiency of heavy metals removal. Increasing the concentration of nanomaterial leads to an increase in the number of active sites. This was studied at different concentrations (1g), (0.5g), and (0.1g), with the highest concentration (1g) recording the highest removal rates, A small amount (0.5–1) of the nanomaterial was used. This method is suitable for small-scale applications, as it achieves high removal efficiency while reducing costs; furthermore, the material can be handled safely and reused, making the process both economical and environmentally friendly[22] .

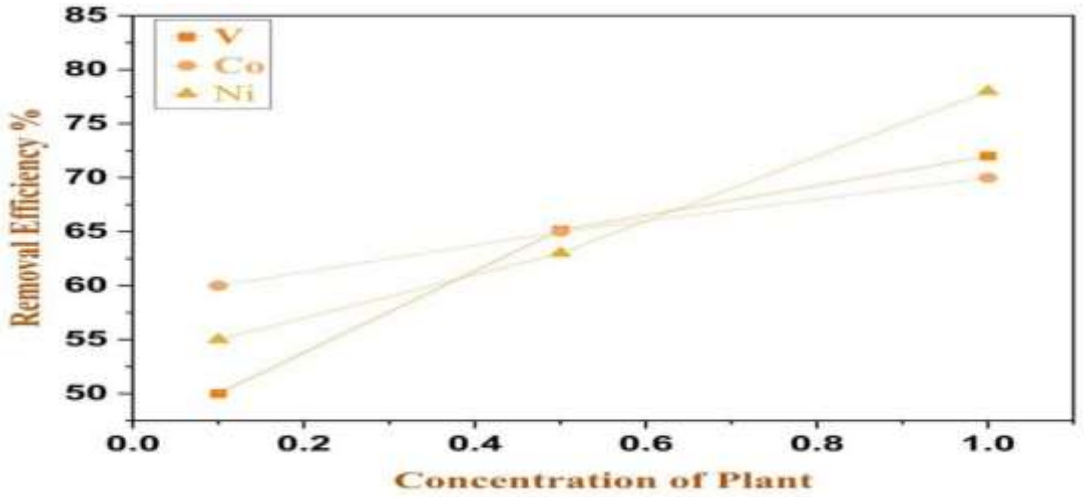


Figure 16. Effect of concentration on metals removal efficiency.

3.5.4. Effect of contact time

The results showed that increasing the contact time between the ions and the nanomaterial provides a greater opportunity for the ions to cross into active sites on the particle surface. The results indicated that a time of 30 min is optimal, at which the removal rate is relatively high[23].

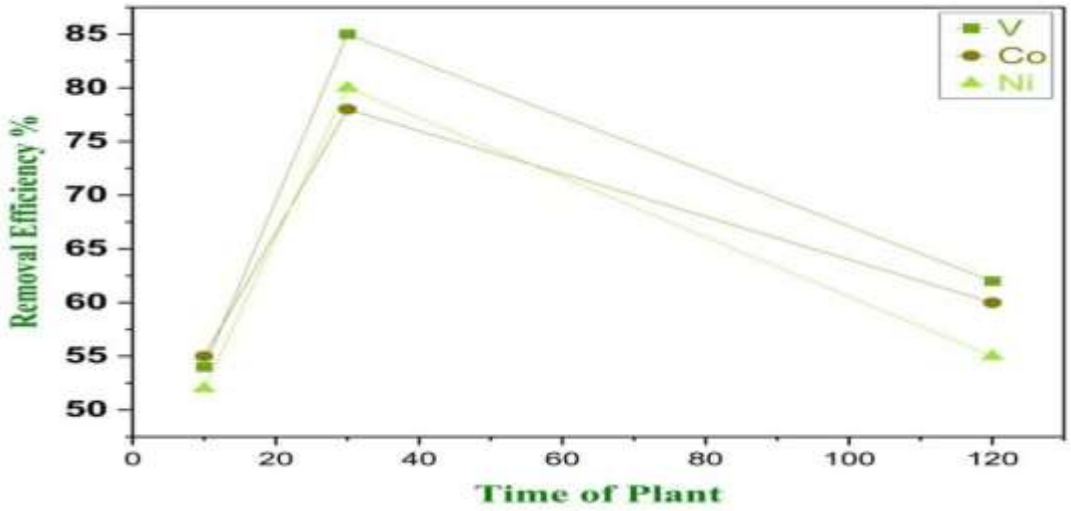


Figure 17. Effect of time on metals removal efficiency.

3.6. Real samples

3.6.1. Removal of heavy metals from water samples using Nano- Adsorbent plant-amine extract

Analysis results revealed variations in removal rates and adsorption efficiency for the heavy metals (Ni^{+2}, Co^{+2}, V^{+5}) across the studied areas: Al-Gharraf, Al-Fadhiliya, and Nasiriyah. The highest removal rate for nickel ions was recorded in Nasiriyah (97.0%) and the lowest in Al-Gharraf (94.5%). Similarly, cobalt ions showed the highest removal rate in Nasiriyah (97.7%) and the lowest in Al-Gharraf (92.3%). For vanadium, the highest removal rate was observed in Nasiriyah (94.7%) and the lowest in Al-Gharraf (92.2%). The results indicated that removal efficiency was highest in Nasiriyah for all studied elements, a finding attributed to differences in water environmental characteristics across the regions. Furthermore, the higher removal efficiency for nickel and cobalt ions compared to vanadium suggests that the nano-adsorbent plant amine possesses more active sites for these specific ions[24,25]. These results align with the study by Padmanabhan (2024) in India, which investigated heavy metal removal from aqueous solutions and plant extracts using amine-based materials; that study reported removal efficiencies exceeding 95% for lead, cadmium, and nickel[5].The removal efficiency (%) of heavy metals was calculated according to the following equation.

Removal Efficiency (%) $= \frac{Ci-Cf}{Ci} * 100$

Where C_i and C_f represent the initial and final concentration (mg/L) of the metal ions before and after adsorption.

Table 4. Estimation of adsorption capacity and removal efficiency of heavy metals in water samples using Nano- Adsorbent plant-amine extract.

Element	Region	C_o	C_e	Q_m	Removal Efficiency(%)
	Al-Gharraf	1.200	0.066	11.34	94.5
Ni^{+2}	Al-Fadhliyya	1.243	0.057	11.68	95.4
	Al-Nasiriyah	1.411	0.039	13.72	97.0
	Al-Gharraf	1.271	0.098	11.73	92.3
Co^{+2}	Al-Fadhliyya	1.278	0.027	12.51	97.3
	Al-Nasiriyah	1.322	0.030	12.92	97.7
	Al-Gharraf	1.214	0.094	11.20	92.2
V^{+5}	Al-Fadhliyya	1.288	0.085	11.94	93.4
	Al-Nasiriyah	1.313	0.070	12.43	94.7

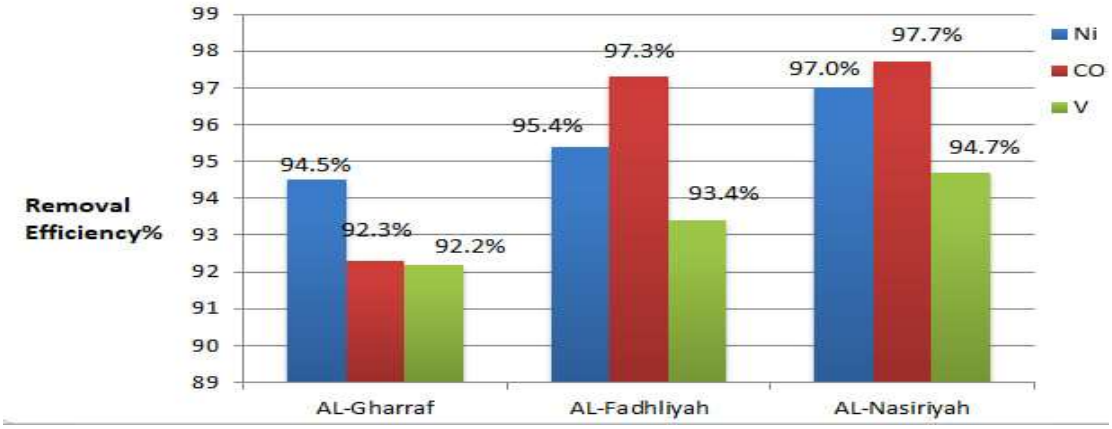


Figure 18. Shows the percentage of heavy metal removal in water samples.

3.6.2. Removal of heavy metals from soil samples using Nano- Adsorbent plant- amine extract

Analysis of soil samples revealed variations in removal rates and adsorption efficiency for the heavy metals (Ni^{2+}, Co^{2+}, V^{5+}) across the studied areas: Al-Gharraf, Al-Fadhiliya, and Nasiriyah. The highest removal rate for nickel ions was observed in Al-Fadhiliya (94.8%), while the lowest was in Al-Gharraf (91.9%). Similarly, cobalt ions showed the highest removal rate in Al-Fadhiliya (94.8%) and the lowest in Al-Gharraf (93.6%). For vanadium, the highest removal rate was recorded in Al-Fadhiliya (91.3%) and the lowest in Al-Gharraf (90%). The results indicated that removal efficiency was highest in the Al-Fadhiliya area for all studied elements, reflecting the influence of soil physicochemical properties on the adsorption process. Furthermore, the lower removal efficiency for vanadium compared to nickel and cobalt ions may be attributed to differences in ionic size and the nature of bonding with the plant extract's nano-surface. This demonstrates the effectiveness of the nano-Adsorbent plant extract in enhancing the adsorption process, despite varying environmental conditions across the regions[26] .

Table 5. Estimation of adsorption capacity and removal efficiency of heavy metals in soil samples using nano-Adsorbent plant- amine extract.

Element	Region	C_o	C_e	Q_m	Removal Efficiency (%)
	Al-Gharraf	1.190	0.096	10.94	91.9
Ni^{+2}	Al-Fadhliyya	1.216	0.066	11.50	94.8
	Al-Nasiriyah	1.270	0.089	11.81	93.0
	Al-Gharraf	1.211	0.077	11.34	93.6
Co^{+2}	Al-Fadhliyya	1.188	0.062	11.24	94.8
	Al-Nasiriyah	1.250	0.065	11.85	94.8
	Al-Gharraf	1.178	0.117	10.71	90.0
V^{+5}	Al-Fadhliyya	1.159	0.100	10.59	91.3
	Al-Nasiriyah	1.189	0.109	10.80	90.8

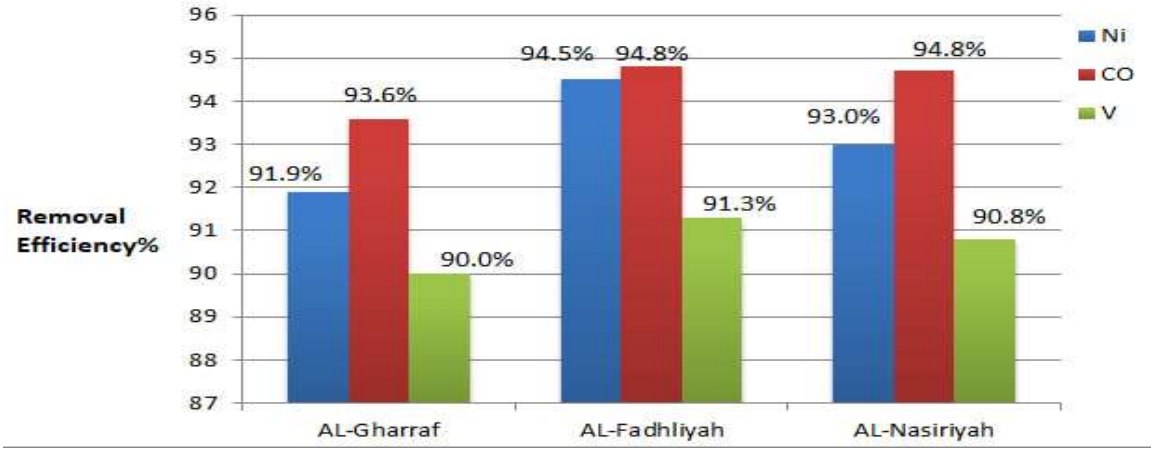


Figure 19. Shows the percentage of heavy metal removal in soil samples**.**

3.6.3. Removal of heavy metals from Plant samples using Nano- Adsorbent plant- amine extract

Analysis of plant samples using the nano-Adsorbent (derived from plant amines) revealed distinct variations in the removal rates and adsorption capacities for heavy metals (Ni^{2+}, Co^{2+}, and V^{5+}) across the Al-Gharraf, Al-Fadhiliya, and Nasiriyah regions; these variations reflect the specific environmental conditions influencing each area. The Nasiriyah region recorded the highest removal rates (96%), while Al-Gharraf recorded the lowest (94.1%). Regarding cobalt ions, Nasiriyah again showed the highest removal rate (96.9%), compared to the lowest rate in Al-Gharraf (96%). Similarly, the highest removal rates for vanadium ions were observed in Nasiriyah (94.8%) and the lowest in Al-Gharraf (91.5%). The results indicated that the Nasiriyah region demonstrated the highest removal efficiency for all studied metals, reflecting the impact of environmental characteristics and growth conditions on the plants in that area. A lower removal rate for vanadium was observed compared to nickel and cobalt; this difference is attributed to the distinct nature of the ions and their interaction with the nano-surface. These findings confirm the effectiveness of the nano-Adsorbent plant amine in enhancing the adsorption process[27].

Table 6. Estimation of adsorption capacity and removal efficiency of heavy metals in Plant samples using Nano-Adsorbent plant-amine extract.

Element	Region	C_o	C_e	Q_m	Removal Efficiency (%)
Ni^{+2}	Al-Gharraf	1.301	0.076	12.25	94.1
	Al-Fadhliyya	1.350	0.061	12.89	95.5
	Al-Nasiriyah	1.321	0.053	12.68	96.0
Co^{+2}	Al-Gharraf	1.330	0.054	12.77	96.0
	Al-Fadhliyya	1.343	0.051	12.92	96.2
	Al-Nasiriyah	1.369	0.043	13.26	96.9
V^{+5}	Al-Gharraf	1.286	0.109	11.77	91.5
	Al-Fadhliyya	1.317	0.099	12.18	92.5
	Al-Nasiriyah	1.327	0.069	12.58	94.8

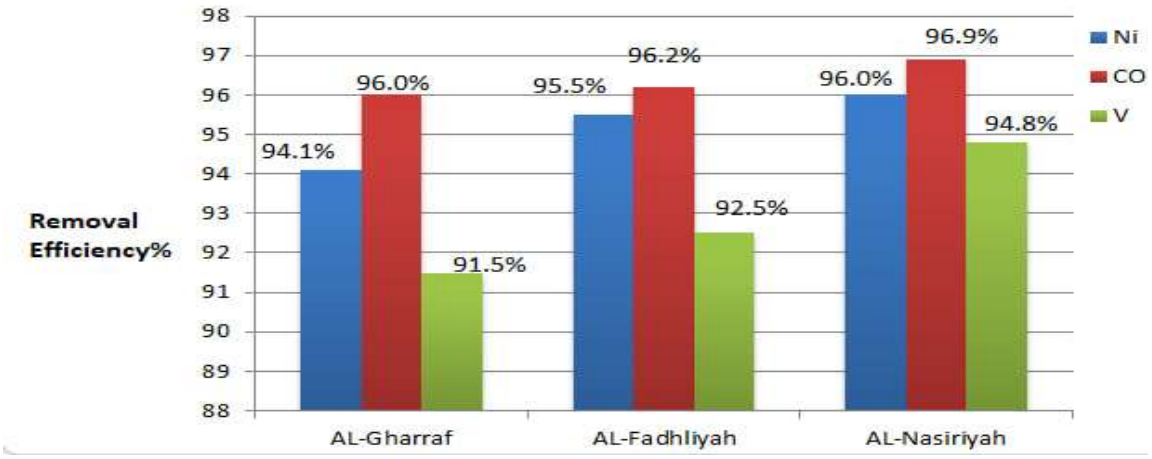


Figure 20. Shows the percentage of heavy metal removal in plant samples.

3.6.4. Removal of heavy metals from herbal extract samples using Nano- Adsorbent plant- amine extract

Analysis of herbal extracts (black tea, fenugreek, and anise) using a nano-Adsorbent material (derived from plant amines) revealed distinct variations in removal rates and adsorption capacities for the heavy metals studied (Ni^{2+}, Co^{2+}, and V^{5+}). Black tea extract demonstrated the highest removal rates for all ions, achieving 98.6% for nickel, 99.4% for cobalt, and 97.4% for vanadium. In contrast, anise extract recorded the lowest rates: 93% for nickel, 94.2% for cobalt, and 93.9% for vanadium, while fenugreek extract showed intermediate efficiency. The results indicate that the high removal efficiency of black tea extract is attributable to its content of active compounds such as polyphenols and tannins which possess a strong capacity to bind with metal ions; conversely, the lower efficiency observed with anise extract may be linked to its chemical composition and a scarcity of active compounds capable of adsorption[28] .

Table 7. Estimation of adsorption capacity and removal ratio of heavy metals in herbal extracts using Nano-Adsorbent plant- amine extract.

Element	Herbal Extract	C_o	C_e	Q_m	Removal Efficiency (%)
Ni^{+2}	Black tea	3.20	0.045	31.55	98.6
	Fenugreek	2.23	0.101	21.29	95.5
	Anise	3.01	0.210	28.01	93.0
Co^{+2}	Black tea	2.59	0.015	25.75	99.4
	Fenugreek	2.26	0.061	21.99	97.3
	Anise	2.73	0.157	25.73	94.2
V^{+5}	Black tea	3.05	0.080	29.70	97.4
	Fenugreek	2.37	0.117	22.53	95.0
	Anise	2.67	0.160	25.08	93.9

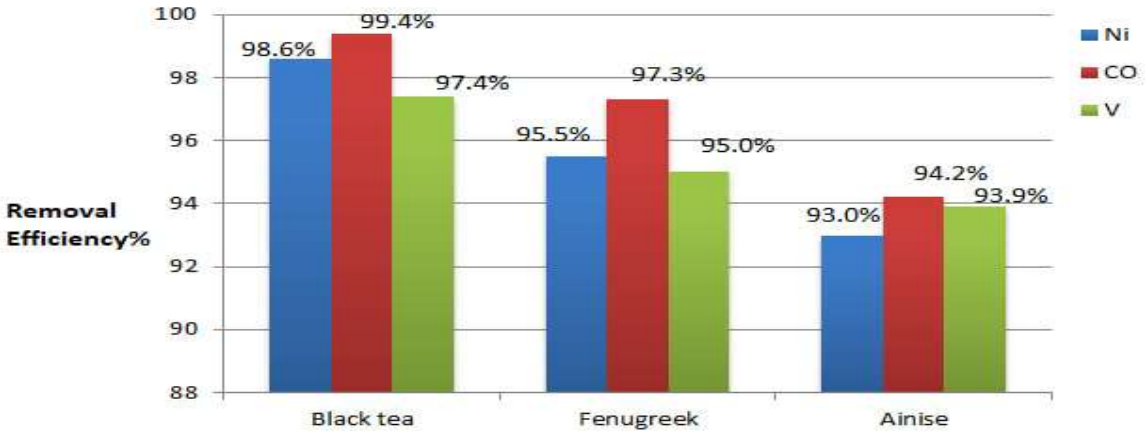


Figure 21. Shows the percentage of heavy metal removal in herbal extract samples.

3.7. Adsorption isotherms

3.7.1. Adsorption of nickel, cobalt and vanadium ions to Nano- Adsorbent amines according to the Langmuir equation

In this study, the Langmuir equation was applied to explain the adsorption of nickel, cobalt, and vanadium ions using a nano-Adsorbent plant- Amine Extract. The Langmuir equation assumes that adsorption occurs in a monolayer on a homogeneous surface, and that all effective adsorption sites are energy-equivalent[29], where the study was conducted according to the Langmuir equation[30]:

$$\frac{Ce}{Qe} = \frac{1}{Qm*b} + \frac{Ce}{Qm}$$

Q_e: Amount of adsorbate adsorbed per unit mass of adsorbent at equilibrium ($mg.g^{-1}$)

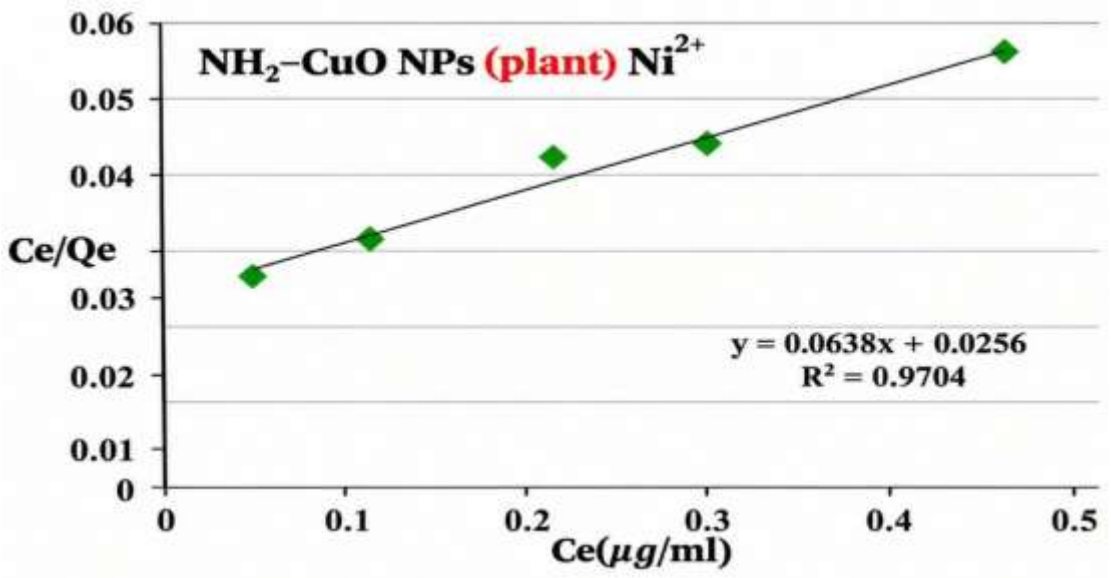
Q_m: Maximum adsorption capacity ($mg.\ g^{-1}$)

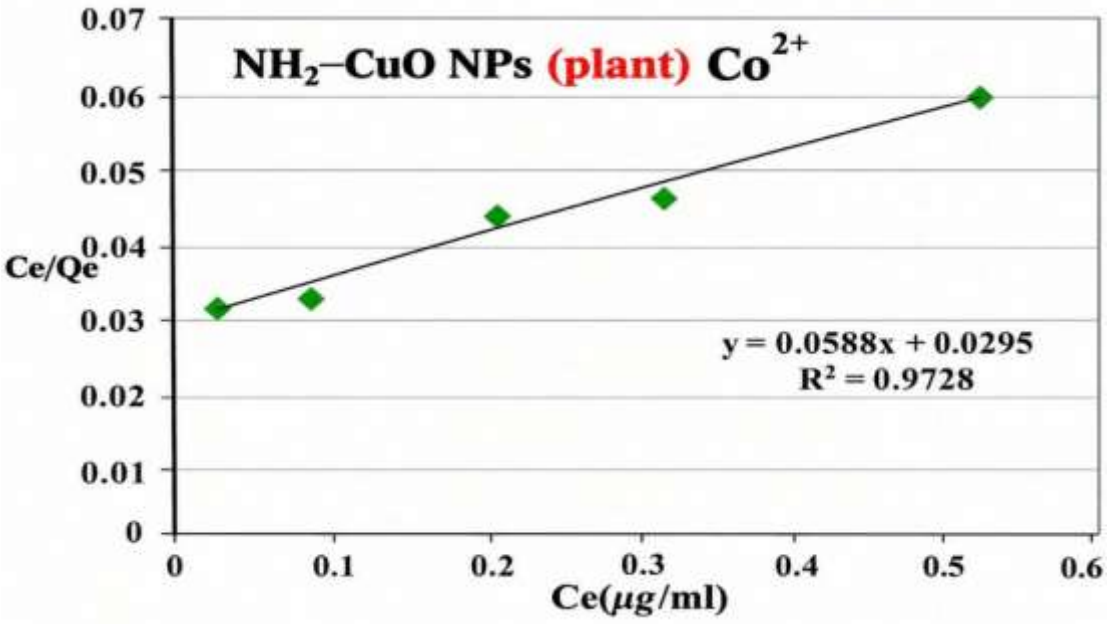
b: Langmuir adsorption constant

C_e: Equilibrium concentration of adsorbate in solution ($mg.\ L^{-1}$)

Table 8. Values for the adsorption of nickel, cobalt, and vanadium ions by nano-Adsorbent plant amines according to the Langmuir equation.

Adsorbent	C_o	Ni^{+2}			Co^{+2}			V^{+5}		
		C_e	Q_e	C_e/Q_e	C_e	Q_e	C_e/Q_e	C_e	Q_e	C_e/Q_e
NH_2-CuO (Nps)	1	0.025	0.097	0.026	0.031	0.969	0.032	0.042	0.958	0.044
	3	0.091	2.909	0.031	0.094	2.906	0.033	0.110	2.890	0.038
	5	0.203	4.797	0.042	0.218	4.782	0.046	0.220	4.780	0.046
	7	0.291	6.709	0.043	0.320	6.680	0.048	0.364	6.636	0.055
	9	0.470	8.530	0.055	0.501	8.499	0.059	0.515	8.485	0.060





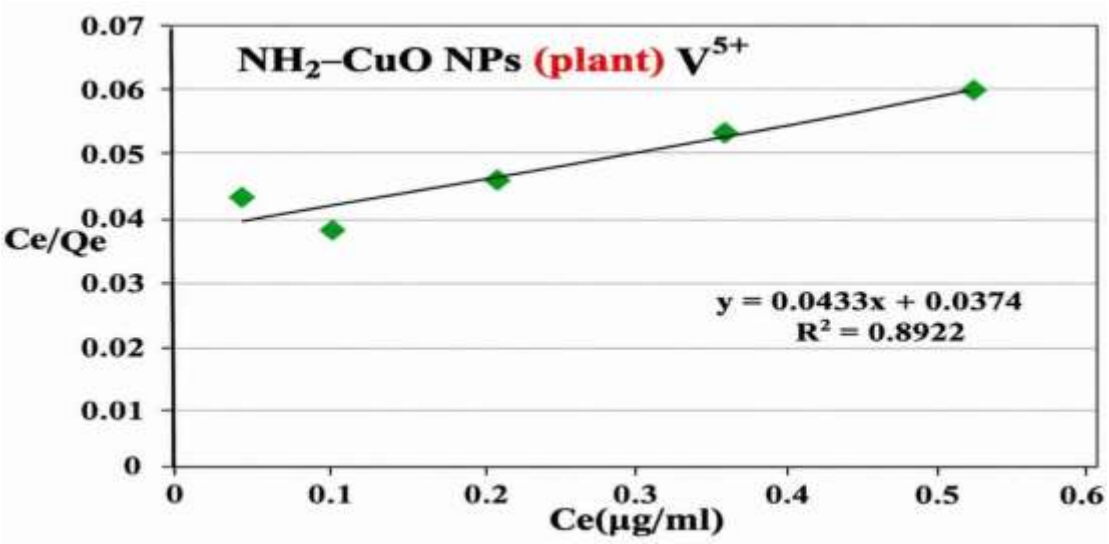


Figure 22. Shows the equation of a straight line and the Langmuir constant.

Table 9. Langmuir constants values.

Element	Adsorbent	Q_m	b	R^2
Ni^{+2}	NH_2-CuO NPs	15.67	1.56	0.9704
CO^{+2}	NH_2-CuO NPs	17.01	1.99	0.9728
V^{+5}	NH_2-CuO NPs	23.09	1.16	0.8922

3.7.2. Adsorption of nickel, cobalt and vanadium ions on Nano-Adsorbent amines according to the freundlich equation

Freundlich's equation assumes that adsorption occurs on a heterogeneous surface with multiple adsorption sites, and the relationship between the equilibrium concentration and the is amount adsorbed expressed as[29] , where the study was conducted according to Freundlich's equation:

$$\textbf{Log } Q_e = \textbf{Log Kf} + \frac{1}{n} * LogCe$$

Q_e: Amount of adsorbate adsorbed per unit mass of adsorbent at equilibrium (mg/g)

Kf: Freundlich constant indicating

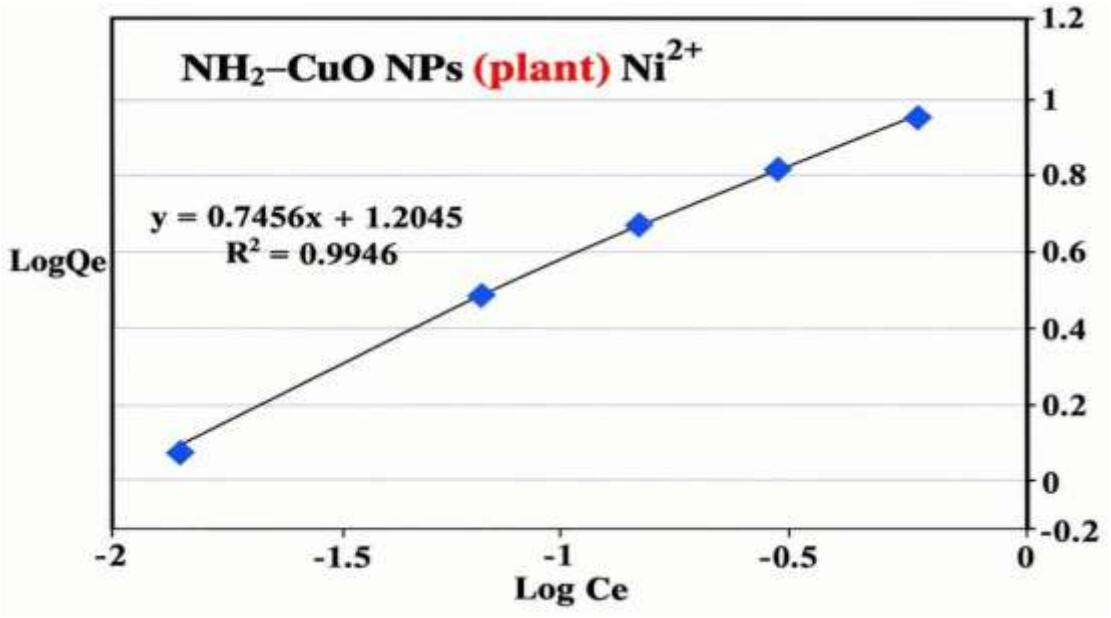
C_e: Equilibrium concentration of adsorbate in solution (mg/L)

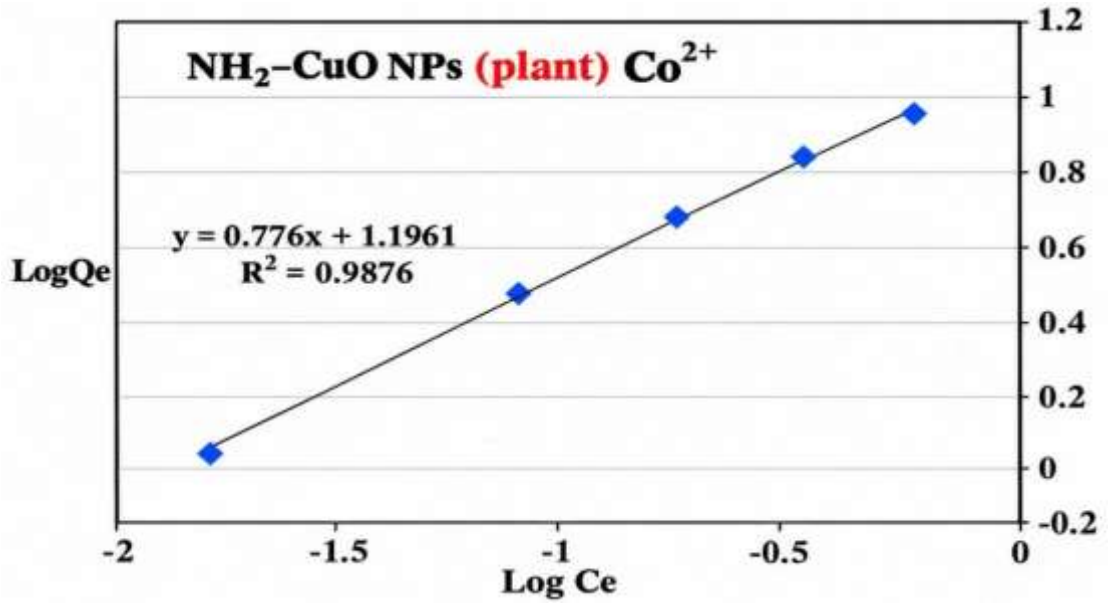
n: Adsorption intensity constant

The high R^2 values indicate that the Freundlich model provides a better fit to the experimental data, demonstrating its suitability for describing the adsorption process under these conditions.

Table 10. Values for the adsorption of nickel, cobalt, and vanadium ions by nano-adsorbent plant amines according to the freundlich equation.

Adsorbent	C_o	Ni^{+2}		Co^{+2}		V^{+5}	
		Log C_e	Log Q_e	Log C_e	Log Q_e	Log C_e	Log Q_e
NH_2-CuO (NPs)	1	-1.602	-0.011	-1.509	-0.014	-1.377	-1.019
	3	-1.041	0.463	-1.027	0.463	-0.959	0.461
	5	-0.693	0.681	-0.661	0.679	-0.658	0.670
	7	-0.536	0.827	-0.495	0.825	-0.438	0.822
	9	-0.328	0.931	-0.300	0.930	-0.288	0.929





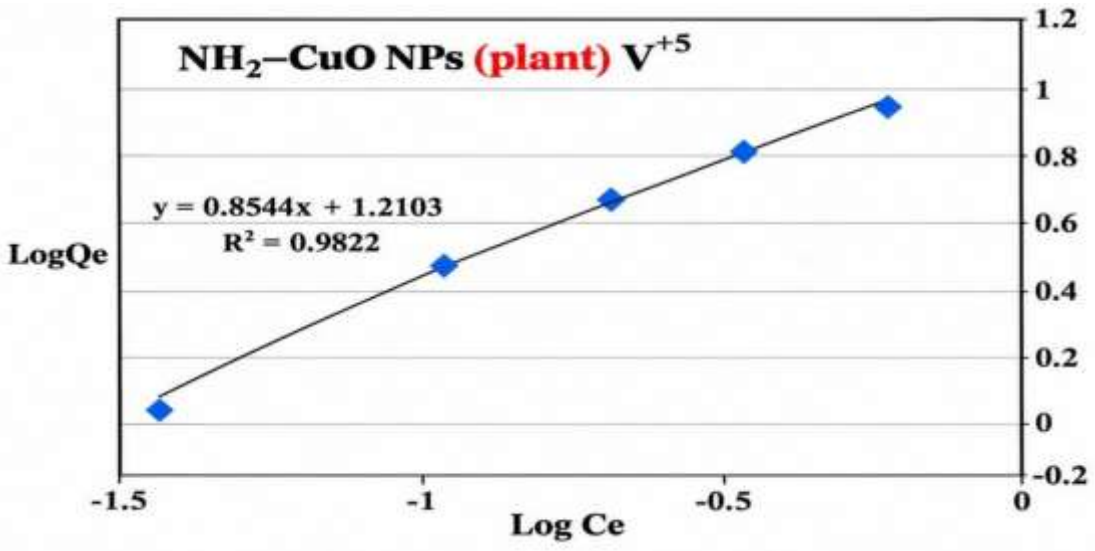


Figure 23. Shows the linear Freundlich.

Table 11. Freundlich constants values.

Element	Adsorbent	n	Kf	R^2
Ni^{+2}	NH_2-CuO NPs	1.34	16.00	0.9946
CO^{+2}	NH_2-CuO NPs	1.29	15.7	0.9876
V^{+5}	NH_2-CuO NPs	1.17	16.2	0.9863

The results of the adsorption isotherm study for nickel, cobalt, and vanadium ions on the adsorbent material (nano-Adsorbent plant-Amine extract) demonstrated that both the Langmuir and Freundlich models describe the data with high accuracy. The R^2 coefficient measures the degree of fit between experimental results and the mathematical model; the closer the value is to one, the more suitable the model. The Freundlich model was found to be the most appropriate for describing the results, as it yielded higher R^2 values. This indicates that the adsorption process occurs on a heterogeneous, multilayered surface and tends to be chemisorption.

3.8. Proposed mechanism on nano-CuO surface

This study elucidates the adsorption mechanism using a nano-adsorbent plant-extract amine. The amine groups serve as active sites that bind to ions such as V^{5+}, Ni^{2+}, and Co^{2+} through coordinate bonding and electrostatic attraction with the nano-CuO surface. These interactions anchor the ions to the surface, thereby enhancing removal efficiency. The results indicate that the surface charge of the material plays a crucial role in the binding process; as the charge varies with the medium's conditions, the strength of the attraction between the surface and the ions is consequently affected[31]

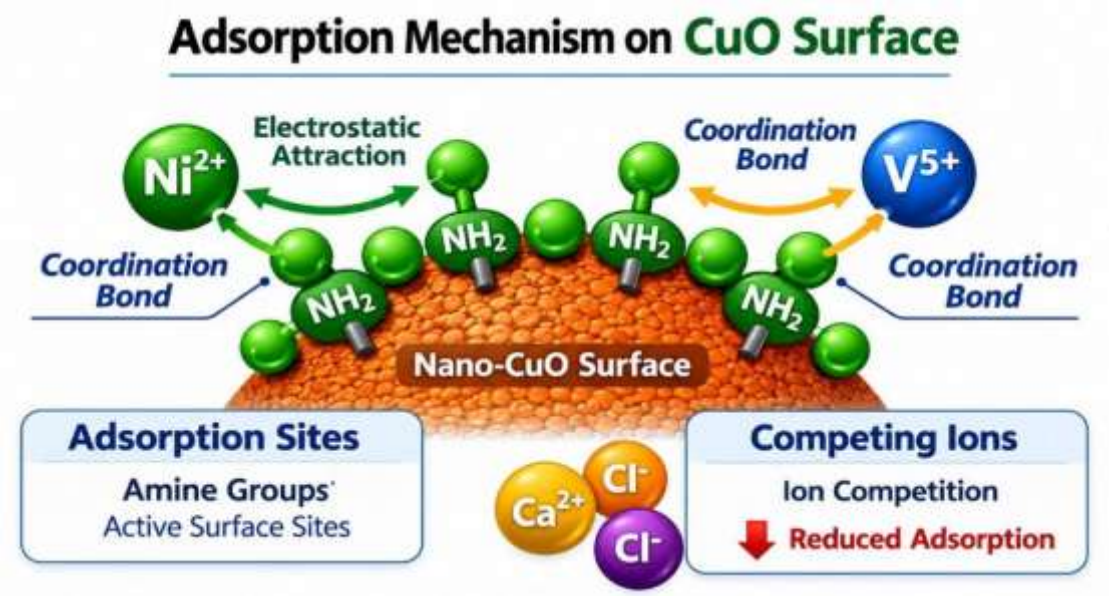


Figure 24. Adsorption mechanism on CuO surface.

3.9. Environmental considerations and safe disposal

The potential environmental risks associated with the accumulation of heavy metal ions on the surface of the nanomaterial were discussed. Strict procedures for safe disposal following hazardous waste protocols were implemented, including chemical treatment and disposal at designated hazardous waste sites. These measures minimize environmental impact and ensure the safe handling of the adsorbent material after use

4. Conclusion

In this study, an efficient and eco-friendly method was developed to synthesize copper oxide nanoparticles (CuO NPs), which were used to modify a plant-Adsorbent amine extracted from the peace lily (Spathiphyllum) to enhance adsorption efficiency. The nano-adsorbent plant amine demonstrated exceptional efficiency in removing heavy metals such as nickel, cobalt, and vanadium from real samples (water, plant, and soil) as well as herbal samples (black tea, fenugreek, and anise). The results indicated that the adsorbent possesses a high adsorption capacity and that the Freundlich model best describes the adsorption process, confirming the data's accuracy and suitability for environmental applications. This approach is not only highly efficient but also safe and environmentally friendly; its potential use in remediating heavy metal pollution opens new avenues for green chemistry applications in environmental protection and the improvement of natural resource quality.

Conflict of interest

The author declares no conflict of interest.

References

1. R. Reddy, R. Appannagari, and D. R. Ramamohana, “Environmental Pollution Causes and Consequences: A Study,” 2017. [Online]. Available: https://www.researchgate.net/publication/323944189.
2. H. Msahir Ateshan, “Studies on Some Heavy Metals Removal inIndustrial and Drinking Water: A review,” *University of Thi-Qar Journal of Science*, vol. 12, no. 2, pp. 34–40, Dec. 2025, doi: 10.32792/utq/utjsci/v12i2.1404.
3. A. N. Ebelegi, N. Ayawei, and D. Wankasi, “Interpretation of Adsorption Thermodynamics and Kinetics,” *Open J. Phys. Chem.*, vol. 10, no. 03, pp. 166–182, 2020, doi: 10.4236/ojpc.2020.103010.
4. B. O. Isiuku, P. C. Okonkwo, and C. D. Emeagwara, “Batch adsorption isotherm models applied in single and multicomponent adsorption systems–a review,” *J. Dispers. Sci. Technol.*, vol. 42, no. 12, pp. 1879–1897, 2021.

5. S. Shintre, S. Kolhe, S. Vidhate, and S. Padmanabhan, “A Simple and Novel Method to Reduce Heavy Metal Contamination from Aqueous Solutions and Herbal Extracts,” 2024. [Online]. Available: www.meddiscoveries.org.
6. G. Ayakdaş and D. Ağagündüz, “Determination of L-Theanine and Caffeine Contents in Tea Infusions with Different Fermentation Degrees and Brewing Conditions Using the Chromatographic Method,” *Foods*, vol. 14, no. 13, Jul. 2025, doi: 10.3390/foods14132313.
7. F. W. Alemu and T. D. Zeleke, “Green synthesis of silver and cobalt oxide nanoparticles using Croton macrostachyus plant extract and evaluation of their antibacterial activity,” *Nanomed. J.*, vol. 11, no. 1, pp. 80–92, Jan. 2024, doi: 10.22038/NMJ.2023.75230.1826.
8. P. J. Sephra, P. Baraneedharan, M. Sivakumar, T. D. Thangadurai, and K. Nehru, “CuO/SiO2 modified amine functionalized reduced graphene oxide with enhanced photocatalytic and electrochemical properties: PJ Sephra et al.,” *SN Appl. Sci.*, vol. 1, no. 1, p. 73, 2019.
9. A. Ahmed and Saher Abdulridha Ali, “Assessment of heavy metals contamination of agricultural soils using pollution indicators in Thi-Qar governorate, Southern Iraq,” *University of Thi-Qar Journal of Science*, vol. 10, no. 2, pp. 20–26, Dec. 2023, doi: 10.32792/utq/utjsci/v10i2.1064.
10. Y. Chen, A. Agrelo-Lestón, I. Burgués-Ceballos, J. Llorca, and L. Soler, “Bimetallic nanoparticles as cocatalysts for photocatalytic hydrogen production,” *Adv. Funct. Mater.*, vol. 36, no. 21, p. e06279, 2026.
11. S. N. Omer *et al.*, “Comparison between green synthesized and commercial copper oxide nanopartifcles against various microorganisms and plant growth of Vigna radiata,” *Sustainable Chemistry for Climate Action*, vol. 6, p. 100073, 2025.
12. H. Hussein Alwan, “IRANIAN JOURNAL OF CATALYSIS Photo Catalysis Desulfurization at Copper Oxides /Titanium Oxide Nanotubes Under UV and Visible Light Irradiation.”
13. M. M. Chikkanna, S. Neelagund, and M. B. Hiremath, “Biological synthesis, characterization and antibacterial activity of novel copper oxide nanoparticles (CuONPs),” *Journal of Bionanoscience*, vol. 12, no. 1, pp. 92–99, Feb. 2018, doi: 10.1166/jbns.2018.1490.
14. A. Yasin *et al.*, “Fabrication of copper oxide nanoparticles using Passiflora edulis extract for the estimation of antioxidant potential and photocatalytic methylene blue dye degradation,” *Agronomy*, vol. 12, no. 10, p. 2315, 2022.
15. R. Chandrasekaran, S. A. Yadav, and S. Sivaperumal, “Phytosynthesis and Characterization of Copper Oxide Nanoparticles using the Aqueous Extract of Beta vulgaris L and Evaluation of their Antibacterial and Anticancer Activities,” *J. Clust. Sci.*, vol. 31, no. 1, pp. 221–230, 2020, doi: 10.1007/s10876-019-01640-6.
16. K. A. Alsoltani and K. H. Harbbi, “Determination microstructure parameters for copper oxide nanoparticles,” in *AIP Conference Proceedings*, AIP Publishing LLC, 2023, p. 020056.
17. T. K. Patle, K. Shrivas, R. Kurrey, S. Upadhyay, R. Jangde, and R. Chauhan, “Phytochemical screening and determination of phenolics and flavonoids in Dillenia pentagyna using UV–vis and FTIR spectroscopy,” *Spectrochim. Acta A Mol. Biomol. Spectrosc.*, vol. 242, p. 118717, 2020.
18. A. Sinha, “Plant-mediated biosynthesis of CuO nanoparticles for photocatalytic organic pollutant degradation (A Review),” *Russ. J. Gen. Chem.*, vol. 95, no. 11, pp. 3177–3204, 2025.
19. S. M. Kheder, H. T. Hussein, and H. M. Al-Attar, “Preparation and characterization of CuO NPs by green synthesis and study of their antimicrobial activity,” in *AIP Conference Proceedings*, AIP Publishing LLC, 2026, p. 050002.
20. M. Malik, K. H. Chan, and G. Azimi, “Quantification of nickel, cobalt, and manganese concentration using ultraviolet-visible spectroscopy,” *RSC Adv.*, vol. 11, no. 45, pp. 28014–28028, 2021.
21. M. Sharma, D. Kumar, and R. Sharma, “Harnessing green nanotechnology and phytoremediation for sustainable mitigation of heavy metals and nanoparticles from wastewater,” *Int. J. Phytoremediation*, pp. 1–36, 2026.
22. M. Pitsikalis, K. Koutras, G. Peppas, E. Pyrgioti, and T. Tsovilis, “Effect of SiC Nanoparticles Size and Concentration on the Partial Discharge Behavior and Dissipation Factor of Synthetic Ester Oil,” in *2025 IEEE Industry Applications Society Annual Meeting (IAS)*, IEEE, 2025, pp. 1–4.
23. V. Manirethan, K. Raval, R. Rajan, H. Thaira, and R. M. Balakrishnan, “Kinetic and thermodynamic studies on the adsorption of heavy metals from aqueous solution by melanin nanopigment obtained from marine source: Pseudomonas stutzeri,” *J. Environ. Manage.*, vol. 214, pp. 315–324, 2018, doi: https://doi.org/10.1016/j.jenvman.2018.02.084.
24. M. Aliyeva, M. Ganibekova, M. Negmatova, D. Gulboyeva, O. Geldiyev, and S. Tursunov, “Removal of metal ions from industrial wastewater with bentonite-modified chitosan Apis mellifera,” in *Advanced Materials for Optics and Photonics: Chemistry and Engineering Perspectives (AMOP 2026)*, SPIE, 2026, pp. 715–724.
25. M. Abatal *et al.*, “Comparison of heavy metals removal from aqueous solution by Moringa oleifera leaves and seeds,” *Coatings*, vol. 11, no. 5, p. 508, 2021.
26. Y. Li, X. Xu, S. Huang, and Z. He, “Study on the remediation of ni-contaminated soil by Fe-Mn modified biochar,” *J. Soils Sediments*, vol. 25, no. 4, pp. 1090–1099, 2025.
27. L. Zhang, T. Zhang, R. Guo, and Y. Si, “Insights into mechanism of jarosite enhanced vanadium (V) bioreduction by Shewanella oneidensis MR-1 and vanadium immobilization in contaminated soil,” *J. Hazard. Mater.*, p. 140961, 2025.

28. K. Y. Foo and B. H. Hameed, “Insights into the modeling of adsorption isotherm systems,” *Chemical engineering journal*, vol. 156, no. 1, pp. 2–10, 2010.
29. J. Wang and X. Guo, “Adsorption isotherm models: Classification, physical meaning, application and solving method,” *Chemosphere*, vol. 258, p. 127279, 2020.
30. S. K. Ajjam, B. H. Hlih, and H. H. Alwan, “Enhancing lead ion removal from simulated wastewater through continuous electrocoagulation process: investigating operating parameters and adsorption behavior,” *Chemical Papers*, 2024, doi: 10.1007/s11696-024-03771-1.
31. J. Wang and X. Guo, “Adsorption isotherm models: Classification, physical meaning, application and solving method,” *Chemosphere*, vol. 258, p. 127279, 2020.